

# Supremacy of the quantum many-body Szilard engine with attractive bosons

J. Bengtsson<sup>1,2</sup>, M. Nilsson Tengstrand<sup>1,2</sup>, A. Wacker<sup>1,2</sup>, P. Samuelsson<sup>1,2</sup>, M. Ueda<sup>4,5</sup>, H. Linke<sup>1,3</sup> & S. M. Reimann<sup>1,2</sup>

<sup>1</sup>NanoLund, Lund University, P.O.Box 118, SE-22100 Lund, Sweden

<sup>2</sup>Mathematical Physics, Lund University, Box 118, 22100 Lund, Sweden

<sup>3</sup>Solid State Physics, Lund University, Box 118, 22100 Lund, Sweden

<sup>4</sup>Department of Physics, University of Tokyo, 7-3-1 Hongo, Bunkyo-ku, Tokyo 113-0033, Japan

<sup>5</sup>RIKEN Center for Emergent Matter Science (CEMS), Wako, Saitama 351-0198, Japan

(Dated: January 30, 2017)

In a classic thought experiment, Szilard [1] suggested a heat engine where a single particle, for example an atom or a molecule, is confined in a container coupled to a single heat bath. The container can be separated into two parts by a moveable wall acting as a piston. In a single cycle of the engine, work can be extracted from the information on which side of the piston the particle resides. The work output is consistent with Landauer's principle that the erasure of one bit of information costs the entropy  $k_B \ln 2$  [2–4], exemplifying the fundamental relation between work, heat and information [5–11]. Here we apply the concept of the Szilard engine to a fully interacting quantum many-body system. We find that a working medium of a number of  $N \geq 2$  bosons with attractive interactions is clearly superior to other previously discussed setups [12–17]. In sharp contrast to the classical case, we find that the average work output increases with the particle number. The highest overshoot occurs for a small but finite temperature, showing an intricate interplay between thermal and quantum effects. We anticipate that our finding will shed new light on the role of information in controlling thermodynamic fluctuations in the deep quantum regime, which are strongly influenced by quantum correlations in interacting systems [18].

## I. INTRODUCTION

The Szilard engine was originally designed as a thought experiment with only a single classical particle [1] to illustrate the role of information in thermodynamics (see, for example, [8] for a recent review). The apparent conflict with the second law could be resolved by properly accounting for the work cost associated with the information processing [2, 3, 19–22]. Although Szilard's suggestion dates back to 1929, only more recently the conversion between information and energy was shown experimentally using a Brownian particle [6]. A direct realisation of the classical Szilard cycle was reported by Roldán *et al.* [23] for a colloidal particle in an optical double-well trap. In a different scenario, Koski *et al.* [24, 25] measured  $k_B T \ln 2$  of work for one bit of information using a single electron moving between two small metallic islands. A quantum version of the single-particle Szilard engine was first discussed by Zurek [26]. In contrast to the classical case, insertion or removal of a wall in a quantum system shifts the energy levels, implying that the process must be associated with non-zero work [27–29]. Kim *et al.* [12] showed that the amount of work that can be extracted crucially depends on the underlying quantum statistics: two non-interacting bosons were found superior to the classical equivalent, as well as to the corresponding fermionic case. Many different facets of the quantum Szilard engine have been studied, including optimisation of the cycle [14, 15] or the effect of spin [16] and parity [17], but all for non-interacting particles. The case of two attractive bosons was discussed in Ref. [13]; however, the authors assigned the increased work output to a classical effect. The question thus remains how the information-to-work conversion in many-body quantum systems is affected by interactions between the particles.

Here, we present a full quantum many-body treatment of spin-0 bosonic particles in a Szilard engine with realistic at-

tractive interactions between the particles, as they commonly occur in, for example, ultra-cold atomic gases [30]. We demonstrate quantum supremacy in the few-body limit for  $N \leq 5$ , where a solution to the full many-body problem can be obtained with very high numerical accuracy. A perturbative approach indicates that the supremacy further increases for larger particle numbers. Surprisingly, the highest overshoot of work compared to  $W_1 = k_B T \ln 2$  (*i.e.*, the highest possible classical work output) occurs for a finite temperature, exemplifying the relation between thermodynamic fluctuations and the many-particle excitation spectrum.

## II. MANY-BODY SZILARD CYCLE FOR BOSONS WITH ATTRACTIVE INTERACTIONS.

Our claim is based on a fully *ab initio* simulation of the quantum many-particle Szilard cycle by exact numerical diagonalisation, *i.e.*, the full configuration interaction method (as further described in the supplementary material). A hard-walled one-dimensional container of length  $L$  confines  $N$  bosons that constitute the working medium. We model the interactions by the usual two-body pseudopotential of contact type [30],  $g\delta(x_1 - x_2)$ , where the strength of the interaction  $g$  is given in units of  $g_0 = \hbar^2/(Lm)$ . The single-particle ground state energy  $E_1 = \hbar^2\pi^2/2mL^2$  sets the energy unit, where  $m$  is the mass of a single particle. The cycle of the Szilard engine goes through four steps, assumed to be carried out quasi-statically and in thermodynamic equilibrium with a single surrounding heat bath at temperature  $T$ : (i) insertion of a wall dividing the quantum many-body system at a position  $\ell^{\text{ins}}$ , followed by (ii) a measurement of the actual particle number  $n$  on the left side of the wall, (iii) reversible translation of the wall to its final position  $\ell_n^{\text{rem}}$  depending on the

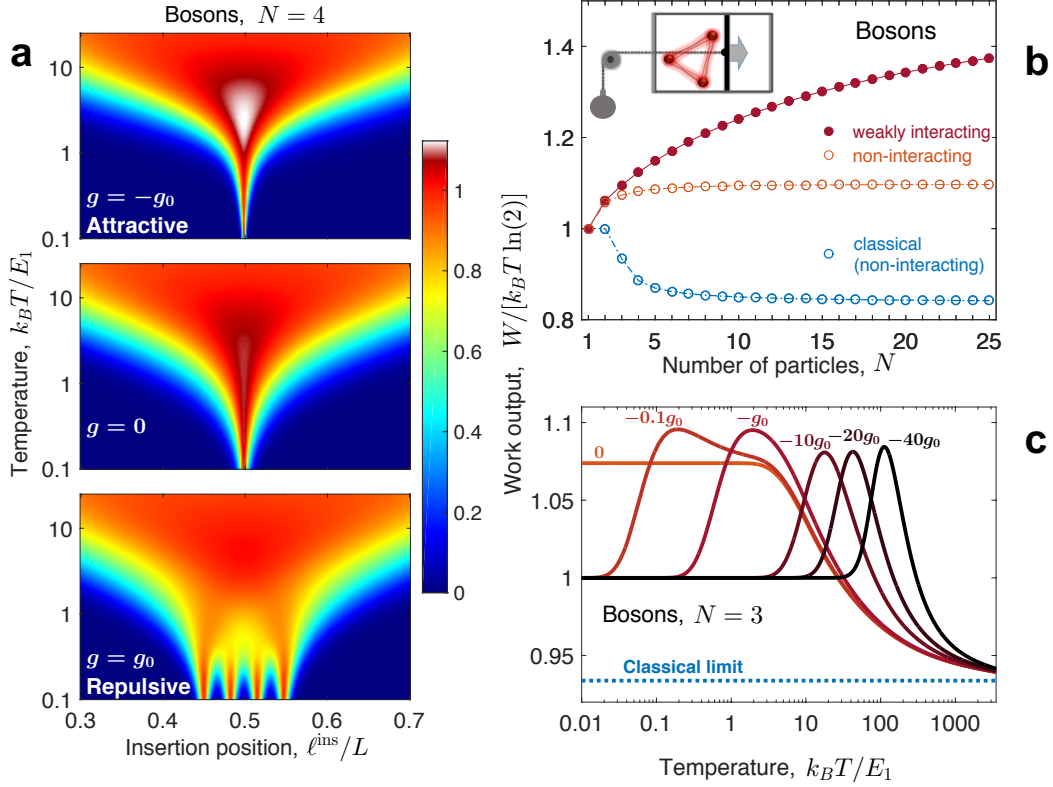


**FIG. 1. Work output of the many-body Szilard engine.** **a** For  $N = 4$  bosons the optimal work output  $W$  (in units of the classical single-particle work  $W_1 = k_B T \ln 2$ ) is found for attractive interactions  $g$  (upper panel) at a finite temperature and around a symmetric insertion position of the barrier. (The interaction strength is in units of  $g_0 = \hbar^2/(Lm)$  with box length  $L$  and single-particle mass  $m$ ). The optimal work output exceeds the case of noninteracting (middle panel) and repulsive bosons (lowest panel). Repulsive bosons exhibit  $N$  peaks in the low-temperature limit for different insertion positions. This behavior is similar to the case of non-interacting fermions and is a signature of the transition into a Tonks-Girardeau state (see text). **b** The maximal work output  $W/W_1$  increases significantly with the particle number for bosons with attractive interactions with  $g = -0.01g_0$ , (solid red line). It is always larger than the result for non-interacting bosons (dashed orange line) and classical particles (dashed blue line). In each case, the temperature is chosen to maximise the relative work output. For non-interacting bosons, this occurs for  $T \rightarrow 0$  (we used  $k_B T/E_1 = 0.01$ ), while the interacting case is optimised at a finite temperature (like the white region in **a**). For classical particles the result is independent of temperature. Optimal insertion and removal positions of the wall are used to maximise  $W/W_1$  for all considered systems. The inset shows a sketch of the many-particle Szilard engine performing work at the expansion step of the cycle. **c** The work output for  $N = 3$  as a function of temperature for different strengths of the attractive interaction. For large  $T$ , all curves converge into the classical result.

outcome  $n$  of the measurement, and finally (iv) removal of the barrier at  $\ell_n^{\text{rem}}$ .

The total average work output of a single cycle with processes (i)-(iv) has been determined [12] as

$$W = -k_B T \sum_{n=0}^N p_n(\ell^{\text{ins}}) \ln \left[ \frac{p_n(\ell^{\text{ins}})}{p_n(\ell_n^{\text{rem}})} \right]. \quad (1)$$

Here,  $p_n(\ell)$  denotes the probability to find  $n$  particles to the left of the wall located at position  $\ell$ , and  $N - n$  particles to the right, if the combined system is in thermal equilibrium. The  $N$ -particle eigenstates  $\Psi_i$  with energy  $E_i$ , obtained by numerical diagonalisation, can be classified by the particle number  $n_i$  in the left subsystem with  $0 < x < \ell$ . Then we find that  $p_n(\ell) = \sum_i \delta_{n_i, n} e^{-E_i(\ell)/k_B T} / Z$  with  $Z = \sum_i e^{-E_i(\ell)/k_B T}$ .

Measuring the particle number on one side after insertion of the wall, one gains the Shannon information [31]  $I =$

$-\sum_{n=0}^N p_n(\ell^{\text{ins}}) \ln p_n(\ell^{\text{ins}})$ . Going back to the original state in the cycle, this information is lost, associated with an average increase of entropy  $\Delta S = k_B I$ . This increase in entropy of the system allows one to extract the average amount of work  $W \leq k_B T I$  which can be positive. Here, the equality only holds if all  $p_n(\ell_n^{\text{rem}}) \equiv 1$ . In this case the removal of the barrier is reversible for each observed particle number. This reversibility had been associated with the conversion of the full information gain into work [32], as explicitly assumed in Ref. [33]. While  $p_n(\ell_n^{\text{rem}}) \equiv 1$  is straightforward for the single-particle case with  $\ell_0^{\text{rem}} = 0$  and  $\ell_1^{\text{rem}} = L$ , this is hard to realise for  $N \geq 2$  [32].

For our case of a moving piston, the full work can typically not be extracted. To optimise  $W$ , we choose the optimal  $\ell_n^{\text{rem}}$ , maximising  $p_n(\ell_n^{\text{rem}})$  for all systems considered here. (The procedure is similar to the non-interacting case [15]).

The highest relative work output is obtained for a many-

body system of *attractive* bosons at a finite temperature. This is the white region in the top panel of Fig. 1 (a), where the work output  $W/W_1 \approx 1.12$  for a system of four attractive bosons surpasses the results for noninteracting (middle panel with  $W/W_1 \lesssim 1.08$ ) as well as for repulsive (lowest panel) bosons. For comparison a system of four classical particles has  $W/W_1 \lesssim 0.886$  (not shown here). We also note that for interaction strengths  $g \leq 0$ , the maximum work output always occurs if the wall is inserted in the middle of the container ( $\ell^{\text{ins}} = L/2$ ) for an engine operating in the deep quantum regime. (For larger temperatures, other insertion positions can become favorable, see the Supplementary Material). For  $T \rightarrow 0$ , the work output vanishes if  $\ell^{\text{ins}} \neq L/2$ . In this limit all non-interacting bosons occupy the lowest single-particle quantum level. After insertion of the wall, the energetically lowest-lying level is in the larger region. For  $\ell^{\text{ins}} \neq L/2$  we know beforehand the location of the particles and measuring the number of particles does not provide any new information, *i.e.*,  $I = 0$ . Consequently, no work can be extracted in the cycle. Attractive interactions obviously enhance this feature. However, this does not hold for repulsive interactions,  $g > 0$ , as shown in the lowest panel of Fig. 1 (a). In this case, the particles spread out on different sides of the wall in the ground state. Here, degeneracies between different many-particle states occur at particular values of  $\ell^{\text{ins}}$ , which allow an information gain in the measurement. This explains the  $N$  distinct peaks as a function of  $\ell^{\text{ins}}$  for low temperature in the lowest panel of Fig. 1 (a).

The maximum of  $W/W_1$  for attractive bosons increases with particle number, as shown in Fig. 1 (b). The optimal relative work output is higher for attractive bosons (*solid red line*) than for non-interacting bosons (*red dashed line*) and clearly beats the corresponding result for classical particles (*blue dashed line*). Here, the data for  $N \leq 5$  were obtained by exact diagonalisation while a perturbative approach (see supplementary material) was applied for  $N > 5$ . The peak work output for bosons with attractive interactions at a finite temperature is a general feature, which holds for a wide range of interaction strengths, see Fig. 1 (c) for the case of  $N = 3$  bosons. Indeed, the temperature at which the peak occurs increases with larger interaction strengths.

### III. ONSET OF THE PEAK AT AN INTERMEDIATE TEMPERATURE.

For systems with attractive interactions,  $g < 0$ , the work output equals  $k_B T \ln 2$  at low temperatures, independent of  $N$ . Due to the dominance of the attractive interaction, all  $N$  particles will be found on one side of the barrier. When the barrier is inserted symmetrically, we have  $p_0(L/2) = p_N(L/2) = 1/2$ , while all other  $p_n(L/2) = 0$ . At the same time, the removal position  $\ell_0^{\text{rem}} = 0$  and  $\ell_N^{\text{rem}} = L$  provide  $p_0(\ell_0^{\text{rem}}) = 1$  and  $p_N(\ell_N^{\text{rem}}) = 1$ , so that Eq. (1) provides the work output  $W = k_B T \ln 2$  for the entire cycle as observed in Fig. 1(c). This case, with two possible measurement outcomes and a full sweep of the piston, resembles the single-particle

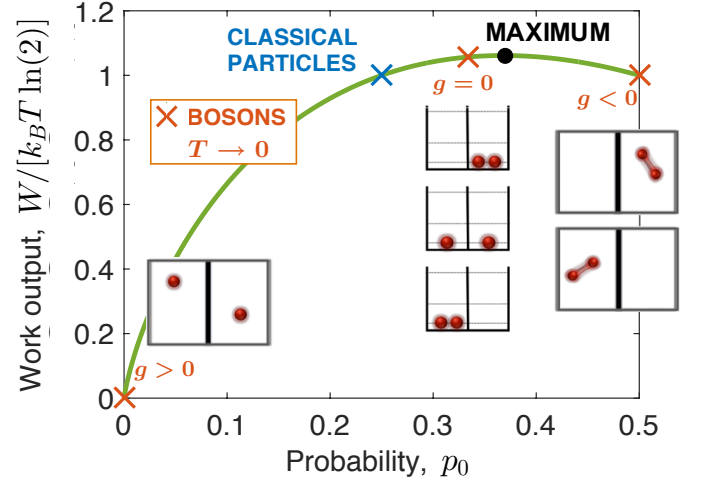


FIG. 2. **Work output per cycle for the two-particle Szilard engine.** For a symmetric insertion of the barrier the work output depends solely on the probability  $p_0$  to find all particles on the right side. For classical particles,  $p_0 = 1/4$  holds, and this result is also reached in all other cases in the limit of high temperatures. However, in the limit of low temperatures,  $p_0$  differs for bosons with different interactions. The insets show the two-particle configurations in the repulsive case (left) and the attractive case (right), as well as the level degeneracy for non-interacting bosons.

case. One might wonder, whether the increased particle number should not imply a higher pressure on the piston and thus, more work. This, however, is not the case, as the attraction between the particles reduces the pressure. Also, when inserting the barrier, the difference in work due to the interactions has to be taken into account. With increasing temperature (*i.e.*,  $k_B T \sim -3g(N-1)/L \approx -0.6(N-1)E_1 g/g_0$ , for weak interactions as shown in the supplementary material) other measurement outcomes than  $n = 0$  or  $n = N$  become probable. Since  $p_0$  and  $p_N$  now decrease with temperature we see a deviation from the performance of the single-particle engine.

### IV. THE TWO-PARTICLE INTERACTING ENGINE.

To get a better understanding of the physics behind the enhancement of work output for bosons with attractive interactions at finite temperatures, let us look at the two-particle case in some more detail. For a central insertion of the barrier, we find  $p_0(L/2) = p_2(L/2)$ . For the same symmetry reasons,  $p_1(\ell)$  has a maximum at this barrier position. No work can thus be extracted in cycles where the two particles are measured on different sides of the central barrier, since  $p_1(\ell^{\text{ins}})/p_1(\ell_1^{\text{rem}}) \geq 1$  in Eq. (1). Thus, the only contributions to the work output result from  $p_0$  and  $p_2$ . Together with  $p_0(\ell_0^{\text{rem}} = 0) = p_2(\ell_2^{\text{rem}} = L) = 1$  we obtain

$$W = -2k_B T p_0(L/2) \ln p_0(L/2) \quad (2)$$

This function has its peak at  $p_0 = 1/e$  with the peak value  $W \approx 1.061 k_B T \ln 2$ , see Fig. 2. This implies a finite value

$p_1 = 1 - 2/e$ . Even if no work can be extracted with one particle on either side of the barrier, a non-zero probability  $p_1$  of such a measurement outcome can be preferable.

Two attractive bosons, initially at  $T \rightarrow 0$  and with  $p_0 = 1/2$ , will for increasing  $T$  continuously approach the classical limit of  $p_0 = 1/4$ . Hence, at a certain temperature, depending on the interaction strength,  $p_0$  passes through  $p_0 = 1/e$  producing a peak in the relative work. Physically, one may understand this property of the engine as follows: At low temperatures, the two attractive bosons will always end up on the same side of the barrier, bound together by their attraction. The cycle is then operating similar to the single particle case, which explains that  $W = k_B T \ln 2$  when  $p_0 = 1/2$ . A less correlated system (obtained with increasing  $T$ ) provides a larger expansion work for cycles in which both particles are on one side of the barrier. On the other hand, cycles with one particle on each side of the barrier, from which no work can be extracted, become more frequent. For  $1/e < p_0 < 1/2$ , the enhanced pressure is more important and the average work output increases with decreasing  $p_0$ . For lower values of  $p_0$ , i.e.  $p_0 < 1/e$ , too few cycles contribute on average to the work production. The average work output decreases with decreasing  $p_0$  despite the corresponding increase in pressure. Importantly, we note the absence of a similar maximum in the non-interacting case, where  $W/W_1$  is found to decrease steadily towards the classical limit with increasing  $T$ .

## V. SZILARD ENGINES WITH $N > 2$ ATTRACTIVE BOSONS.

The maximum of  $W/W_1$  tends to increase with the particle number  $N$  (as previously discussed in connection with Fig. 1 b). The reason lies in the fact that work can be extracted from a larger number of measurement outcomes. Similar to the two-particle engine, the combined contribution to the average work output from cycles in which all particles are on the same side of a barrier inserted at  $\ell^{\text{ins}} = L/2$  is given by Eq. (2). However, also cycles with  $n = 1, 2, \dots, N-1$  (except if  $n = N/2$ ) on the left side of the barrier do contribute to the average work output, and work output even higher than in the two-particle case is possible. The maximum of  $p_1(\ell)$  and that of  $p_{N-1}(\ell)$  occurs for  $\ell \neq L/2$ , as clearly indicated by the probabilities for different measurement outcomes shown for  $N = 4$  in Fig. 3. This means that  $p_n(\ell^{\text{ins}})/p_n(\ell_n^{\text{rem}}) \leq 1$  is possible for  $\ell^{\text{ins}} = L/2$  and that work may be extracted in agreement with Eq. (1). For all systems considered here, with insertion of the barrier at the midpoint the optimum is reached for  $p_0 = p_N \approx 0.3$  (see the example for  $N = 4$  in Fig. 3), which is close to the optimal value of  $1/e$  for the corresponding two-particle engine.

## VI. REPULSIVE BOSONS

Finally, we consider the repulsive interactions between bosons, see Figure 1(c). In the low-temperature limit, the relative work output is very similar to that of non-interacting

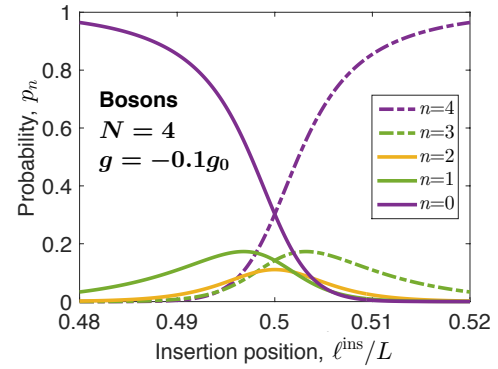


FIG. 3. **Probability distributions.** Work can be extracted in all cycles with insertion of the wall at the midpoint, except for the case with equally many particles on either side. Shown are the probability distributions assigned to the different measurement outcomes at the temperature of the maximal relative work output ( $k_B T/E_1 \approx 0.243$ ) for  $N = 4$  bosons with weak attraction,  $g = -0.1g_0$ .

spin-less fermions discussed in Refs. [13, 14]. This resemblance becomes even more pronounced with increasing interaction strength. This in fact is no coincidence, but rather a property of one-dimensional bosons with strong, repulsive interactions that have an impenetrable core: Indeed, in the limit of infinite repulsion, bosons act like spin-polarised non-interacting fermions. This is the well-known Tonks-Girardeau regime [34]. Both for non-interacting fermions and strongly repulsive bosons, the region where the quantum Szilard engine exceeds the classical single-particle maximum of work output, has disappeared.

## VII. CONCLUSIONS

We have demonstrated that the work output of the quantum Szilard engine can be significantly boosted by short-ranged attractive interactions for a bosonic working medium. We based our claim on the (numerically) exact solution of the full many-body Schrödinger equation for up to five bosons. It is likely that the effect is even further enhanced for larger particle numbers; however, despite the simple one-dimensional setup, the numerical effort grows very significantly (and beyond our feasibility) for larger  $N$ . By increasing the strength of the inter-particle attraction, the engine's work output can be increased significantly also at higher temperatures, where the work that can be extracted generally is of larger magnitude. While we here restrict our analysis to idealised quasi-static processes, it would be of much interest to consider a finite speed in the ramping of the barrier, enabling transitions to excited states which by coupling to baths will lead to dissipation. Extending our approach to quantify irreversibility in real processes on the basis of a fully *ab initio* quantum description may in the future allow to study dissipative aspects in the kinetics of the conversion between information and work.



- 
- [1] Szilard, L. Über die entropieverminderung in einem thermodynamischen system bei eingriffen intelligenter wesen. *Z. Phys.* **53**, 840–856 (1929).
  - [2] Landauer, R. Irreversibility and heat generation in the computing process. *IBM J. Res. Dev.* **5**, 183–191 (1961).
  - [3] Bennett, C. H. The thermodynamics of computation—a review. *International Journal of Theoretical Physics* **21**, 905–940 (1982).
  - [4] Leff, H. S. & Rex, A. F. *Maxwell’s Demon 2: Entropy, Classical and Quantum Information Computing* (IOP Publishing, Bristol, 2003).
  - [5] Maruyama, K., Nori, F. & Vedral, V. *Colloquium* : The physics of Maxwell’s demon and information. *Rev. Mod. Phys.* **81**, 1–23 (2009).
  - [6] Toyabe, S., Sagawa, T., Ueda, M., Muneyuki, E. & Sano, M. Experimental demonstration of information-to-energy conversion and validation of the generalized jarzynski equality. *Nature Physics* **6**, 988–992 (2010).
  - [7] Eisert, J., Friesdorf, M. & Gogolin, C. Quantum many-body systems out of equilibrium. *Nat Phys* **11**, 124–130 (2015).
  - [8] Parrondo, J. M. R., Horowitz, J. M. & Sagawa, T. Thermodynamics of information. *Nat Phys* **11**, 131–139 (2015).
  - [9] Lutz, E. & Ciliberto, S. Information: From maxwells demon to landauers eraser. *Physics Today* **58**, 30 (2015).
  - [10] Quan, H. T., Liu, Y.-x., Sun, C. P. & Nori, F. Quantum thermodynamic cycles and quantum heat engines. *Phys. Rev. E* **76**, 031105 (2007).
  - [11] Uzdin, R., Levy, A. & Kosloff, R. Equivalence of quantum heat machines, and quantum-thermodynamic signatures. *Phys. Rev. X* **5**, 031044 (2015).
  - [12] Kim, S. W., Sagawa, T., De Liberato, S. & Ueda, M. Quantum Szilard engine. *Phys. Rev. Lett.* **106**, 070401 (2011).
  - [13] Kim, K.-H. & Kim, S. W. Szilard’s information heat engines in the deep quantum regime. *J. Korean Phys. Soc.* **61**, 1187–1193 (2012).
  - [14] Cai, C. Y., Dong, H. & Sun, C. P. Multiparticle quantum szilard engine with optimal cycles assisted by a maxwell’s demon. *Phys. Rev. E* **85**, 031114 (2012).
  - [15] Jeon, H. J. & Kim, S. W. Optimal work of the quantum szilard engine under isothermal processes with inevitable irreversibility. *New J. Phys.* **18**, 043002 (2016).
  - [16] Zhuang, Z. & Liang, S.-D. Quantum szilard engines with arbitrary spin. *Phys. Rev. E* **90**, 052117 (2014).
  - [17] Lu, Y. & Long, G. L. Parity effect and phase transitions in quantum szilard engines. *Phys. Rev. E* **85**, 011125 (2012).
  - [18] Perarnau-Llobet, M. *et al.* Extractable work from correlations. *Phys. Rev. X* **5**, 041011 (2015).
  - [19] Piechocinska, B. Information erasure. *Phys. Rev. A* **61**, 062314 (2000).
  - [20] Plenio, M. & Vitelli, V. The physics of forgetting: Landauers erasure principle and information theory. *Contemp. Phys.* **42**, 25–60 (2001).
  - [21] Sagawa, T. & Ueda, M. Second law of thermodynamics with discrete quantum feedback control. *Phys. Rev. Lett.* **100**, 080403 (2008).
  - [22] Sagawa, T. & Ueda, M. Minimal energy cost for thermodynamic information processing: Measurement and information erasure. *Phys. Rev. Lett.* **102**, 250602 (2009).
  - [23] Roldan, E., Martinez, I. A., Parrondo, J. M. R. & Petrov, D. Universal features in the energetics of symmetry breaking. *Nat Phys* **10**, 457–461 (2014).
  - [24] Koski, J. V., Maisi, V. F., Pekola, J. P. & Averin, D. V. Experimental realization of a szilard engine with a single electron. *Proc. Natl. Acad. Sci.* **111**, 13786–13789 (2014).
  - [25] Koski, J. V., Kutvonen, A., Khaymovich, I. M., Ala-Nissila, T. & Pekola, J. P. On-chip maxwell’s demon as an information-powered refrigerator. *Phys. Rev. Lett.* **115**, 260602 (2015).
  - [26] Zurek, W. H. Maxwell’s demon, Szilard’s engine and quantum measurements. In Moore, G. T. & Scully, M. O. (eds.) *Frontiers of Nonequilibrium Statistical Physics*, 151–161 (Springer US, Boston, MA, 1986).
  - [27] Bender, C. M., Brody, D. C. & Meister, B. J. Unusual quantum states: non-locality, entropy, maxwell’s demon and fractals. *Proc. R. Soc. London A: Mathematical, Physical and Engineering Sciences* **461**, 733–753 (2005).
  - [28] Gea-Banacloche, J. Splitting the wave function of a particle in a box. *Am. J. Phys.* **70**, 307–312 (2002).
  - [29] Gea-Banacloche, J. & Leff, H. S. Quantum version of the szilard one-atom engine and the cost of raising energy barriers. *Fluctuation and Noise Letters* **05**, C39–C47 (2005).
  - [30] Bloch, I., Dalibard, J. & Zwerger, W. Many-body physics with ultracold gases. *Rev. Mod. Phys.* **80**, 885–964 (2008).
  - [31] Shannon, C. E. A mathematical theory of communication. *Bell Syst. Tech. J.* **27**, 379–423 (1948).
  - [32] Horowitz, J. M. & Parrondo, J. M. R. Designing optimal discrete-feedback thermodynamic engines. *New J. Phys.* **13**, 123019 (2011).
  - [33] Plesch, M., Dahlsten, O., Goold, J. & Vedral, V. Maxwell’s daemon: Information versus particle statistics. *Sci. Rep.* **4**, 6995 EP – (2014).
  - [34] Girardeau, M. Relationship between systems of impenetrable bosons and fermions in one dimension. *J. Math. Phys.* **1**, 516–523 (1960).
  - [35] De Boor, C. *A practical guide to splines; rev. ed.* Applied mathematical sciences (Springer, Berlin, 2001).
  - [36] Guckenheimer, J. & Holmes, P. J. *Nonlinear Oscillations, Dynamical Systems, and Bifurcations of Vector Fields* (Springer, Berlin, 1983).

## Supplementary Material

### 1. Work output of the quantum Szilard engine

In contrast to other conventional heat engines that operate by exploiting a temperature gradient, as discussed in many textbooks on thermodynamics, the Szilard engine [1] allows for work to be extracted also when connected to a *single* heat bath at constant temperature. It is propelled by the information obtained about the working medium and its microscopical properties. In the supplementary material, we briefly outline the theoretical description of the quantum Szilard engine, in close analogy to that of Refs. [12, 15]. An idealised version of the Szilard engine cycle consists of four well-defined steps: (i) *insertion*, (ii) *measurement*, (iii) *expansion* and finally (iv) *removal*. First, an impenetrable barrier is introduced (i) that effectively splits the working medium into two halves. Then, the number of particles on each side of the barrier is measured (ii). Depending on the outcome of this measurement, the barrier moves (iii) to a new position and contraction-expansion work can be extracted in the process. Finally, the barrier is removed (iv) which completes a single cycle of the engine.

All four steps, (i)-(iv), of the Szilard engine are assumed to be carried out quasi-statically and in thermodynamic equilibrium with a surrounding heat bath at temperature  $T$ . Now, the work associated with an isothermal process can be obtained from

$$W \leq -\Delta F = k_B T \Delta (\ln Z), \quad (3)$$

where  $k_B$ ,  $F$  and  $Z$  are the Boltzmann constant, the Helmholtz free energy and the partition function

$$Z = \sum_j e^{-E_j/(k_B T)}, \quad (4)$$

where the sum runs over the energies  $E_j$  of, in principle, all micro (or quantum) states of the considered system. In practice, however, we construct an approximate partition function from a finite number of energy states. Note that the work in Eq. (3) is chosen to be positive if done *by* the system. Also, the equivalence between  $W$  and  $-\Delta F$  is reserved for reversible processes alone.

We now turn to the work associated with the individual steps of the quantum Szilard engine. For simplicity, we consider an engine with  $N$  particles initially confined in a one-dimensional box of size  $L$ . All steps of the engine are, as previously mentioned, carried out quasi-statically and in thermal equilibrium with the surrounding heat bath at temperature  $T$ . To maximise the work output, we further assume that all involved processes are reversible, unless specified otherwise.

(i) *Insertion*. A wall is slowly introduced at  $\ell^{\text{ins}}$ , where  $0 \leq \ell^{\text{ins}} \leq L$ . In the end, the initial system is divided into left and right sub-systems of sizes  $\ell^{\text{ins}}$  and  $L - \ell^{\text{ins}}$  respectively. Based on Eq. (3), the work of this process is given by

$$W_{(i)} = k_B T \ln \left[ \frac{\sum_{n=0}^N Z_n(\ell^{\text{ins}})}{Z_N(L)} \right], \quad (5)$$

where  $Z_n(\ell^{\text{ins}})$  is the short-hand notation for the partition function obtained with  $n$  particles in the left sub-system and

$N - n$  in the right one. With this notation,  $Z_N(L)$  is thus equivalent to the partition function of the initial system, before the insertion of the barrier. Also, note that prior to measurement, the number of particles on either side of the barrier is not yet a characteristic property of the new system. We need thus to sum over all possible particle numbers in the numerator of Eq. (5). Finally, we want to stress the fact that, unlike for a classical description of the engine, the insertion of a barrier costs energy in the form of work, due to the associated change in the potential landscape.

(ii) *Measurement*. The number of particles located on the different sides of the barrier is now measured. Here, following [13], we assume that the measurement process itself costs no work, *i.e.*, we assume that  $W_{(ii)} = 0$  (see main text). The probability that  $n$  particles are measured to be on the left side of the barrier (and  $N - n$  on the right side) is given by

$$p_n(\ell^{\text{ins}}) = \frac{Z_n(\ell^{\text{ins}})}{\sum_{n'=0}^N Z_{n'}(\ell^{\text{ins}})}. \quad (6)$$

(iii) *Expansion*. The barrier introduced in (i) is assumed to move without friction. During this expansion/contraction process, the number of particles on either side of the barrier remains fixed. In other words, the barrier is assumed high enough such that tunnelling may be neglected. If the barrier moves from  $\ell^{\text{ins}}$  to  $\ell_n^{\text{rem}}$  when  $n$  particles are measured in the left sub-system, the average work extracted from this step of the cycle reads

$$W_{(iii)} = k_B T \sum_{n=0}^N p_n(\ell^{\text{ins}}) \ln \left[ \frac{Z_n(\ell_n^{\text{rem}})}{Z_n(\ell^{\text{ins}})} \right], \quad (7)$$

where  $p_n$  are the probabilities given by Eq. (6).

(iv) *Removal*. The barrier at  $\ell_n^{\text{rem}}$ , that separates the left sub-system with  $n$  particles from the right one with  $N - n$  particles, is now slowly removed. As the height of the barrier shrinks, particles will eventually start to tunnel between the two sub-systems. This transfer of particles makes the removal of the barrier an irreversible process. Clearly, if we instead were to start without a barrier and introduce one at  $\ell_n^{\text{rem}}$ , then we can generally not be certain to end up with  $n$  particles to the left of the partitioner. Assuming that the particles are fully delocalised between the two sub-systems already in the infinite height barrier limit, then the average work associated with the removal process is given by

$$W_{(iv)} = k_B T \sum_{n=0}^N p_n(\ell^{\text{ins}}) \ln \left[ \frac{Z_N(L)}{\sum_{n'=0}^N Z_{n'}(\ell_n^{\text{rem}})} \right]. \quad (8)$$

Finally, the averaged combined work output of a single Szilard cycle,  $W$ , is given by the sum of the partial works associated with the four steps (i)-(iv), *i.e.*  $W = W_{(i)} + W_{(ii)} + W_{(iii)} + W_{(iv)}$ , and simplifies into

$$W = -k_B T \sum_{n=0}^N p_n(\ell^{\text{ins}}) \ln \left[ \frac{p_n(\ell^{\text{ins}})}{p_n(\ell_n^{\text{rem}})} \right]. \quad (9)$$

which is the central equation (1) in the main article.

## 2. The interacting many-body Hamiltonian and exact diagonalisation

To keep the schematic setup of the many-body Szilard cycle as simple as possible, we consider a quantum system of  $N$  interacting particles, initially confined in a one-dimensional box of size  $L$  that is separated by a barrier inserted at a certain position  $\ell$ . We note that for contact interactions between the particles, as defined in the main text, the exact energies  $E_j$  to the fully interacting many-body Hamiltonian  $\hat{H}$  are those given in terms of two independent systems with  $n$  and  $N - n$  particles. In order to construct the partition functions and compute the probabilities  $p_n$ , the entire exact many-body energy spectrum is needed. For the simple case of non-interacting particles (or single-particle systems) these energies are known analytically. For interacting particles, however, they must be determined by solving the full many-body problem. We here apply the configuration interaction method where we use a basis of the 5th order B-splines [35], with a linear distribution of knot-points within each left/right sub-system, to determine the energies of each sub-system and parity at each stage. For  $N = 3$ , we used 62 B-splines (or one-body states) to construct the many-body basis for each sub-system. Since the dimension of the many-body problem grows drastically with  $N$ , we needed to decrease the number of B-splines to 32 for  $N = 4$ . Consequently, in this case we could not go to equally high temperatures and interaction strengths.

## 3. Perturbative approach for weakly attractive bosons at low temperatures

Here we consider the case  $k_B T \ll E_1$ , so that only the lowest quantum levels in each part are thermally occupied. In the case of vanishing interaction, the state with  $n$  particles in the lowest level of the left part of the wall positioned at  $\ell$  (and  $N - n$  particles in the lowest level of the right part) has the energy

$$E_n^{(0)}(\ell) = nE_1 \left( \frac{L}{\ell} \right)^2 + (N - n)E_1 \left( \frac{L}{L - \ell} \right)^2$$

Applying the wave function  $\Psi_0(x) = \sin(\pi x/\ell)\sqrt{2/\ell}$  for the left side, the mutual interaction energy between two particles in this level is

$$U(\ell) = g \int_0^\ell dx |\Psi_0(x)|^4 = \frac{3g}{2\ell} \quad (10)$$

Now we assume that this interaction energy (times the number of interacting partners) is much smaller than the level spacing, i.e.  $(n - 1)U(\ell) \ll 3E_1 \left( \frac{L}{\ell} \right)^2$ , which is satisfied for  $g \ll \frac{\pi^2 g_0}{N-1}$ . Then we may determine the energy of the many-particle state by first-order perturbation theory. This results in the interaction energy

$$E_n^{(1)}(\ell) = \frac{n(n-1)}{2} U(\ell) + \frac{(N-n)(N-n-1)}{2} U(L-\ell). \quad (11)$$

Setting  $E_n(\ell) \approx E_n^{(0)}(\ell) + E_n^{(1)}(\ell)$ , we obtain an analytical expression for the probabilities  $p_n(\ell)$  without any need for

numerical diagonalisation. Using  $\ell^{\text{ins}} = L/2$  and determining the optimal removal positions  $\ell_n^{\text{rem}}$  numerically, we get the work output by Eq. (1). Again the optimal temperature needs to be chosen to obtain the results plotted in Fig. 1(b).

## 4. Estimate of the peak temperature

For the symmetric wall position, the ground state of the system with attractive bosons has all particles on one side, say the left one. Using the perturbative approach discussed above, the interaction energy is  $E_N^{(1)}(L/2)$ . If one boson is transferred from the left side to the right side, the interaction energy changes to  $E_{N-1}^{(1)}(L/2)$ , while the level energies  $E_n^{(0)}(L/2)$  are independent on  $n$  for the symmetric wall position. Thus thermal excitations become likely for  $k_B T \sim E_{N-1}^{(1)}(L/2) - E_N^{(1)}(L/2) = -3(N-1)g/L$ . For these temperatures the particles do not cluster on the same side of the wall any longer and we have  $p_0 < 1/2$ .

## 5. Temperature dependence of the work output for different interaction strengths

As a complement to Fig. 1(c) of the main article, we show the case for  $N = 4$  here in Fig. 4. For small to medium couplings  $-g_0 \lesssim g < 0$ , the peaks have approximately the same height and they are shifted proportionally to  $g$ . This shift follows the deviations from the low temperature limit  $W = W_1$ , which set in at  $k_B T \approx -0.6(N-1)E_1 g/g_0$ , as shown by the approximative approach in the main article. As discussed in the method section, for  $g \approx -\pi^2 g_0/(N-1)$ , correlation effects become important and we find a reduced peak at  $g = -10g_0$ , similar to the case for  $N = 3$  in Fig. 1(c) of the main article. Due to the high numerical demand on the numerical diagonalization, we did not obtain results for larger  $|g|$  in the case  $N = 4$ , while for  $N = 3$  an increase of the peak height for even larger  $|g|$  is observed.

For all interaction strengths  $g < 0$ , the peak height is actually larger than the peak for the attractive two-particle case  $W_2 \approx 1.061 k_B T \ln(2)$  depicted in Fig. 2 of the main article. This is due to the fact, that Eq. (2) of the main article is a lower bound for the work output and  $p_0(L/2)$  necessarily moves from  $1/2$  at  $T \rightarrow 0$  to the classical result  $1/2^N$  at large temperatures. Thus the maximum for  $p_0 = 1/e$  is taken at some intermediate temperature.

## 6. Operation of the Quantum Szilard engine at high temperatures

For  $N = 4$  particles, Fig. 5 shows that the symmetric insertion point  $\ell^{\text{ins}} = L/2$  is not optimal for high temperatures.

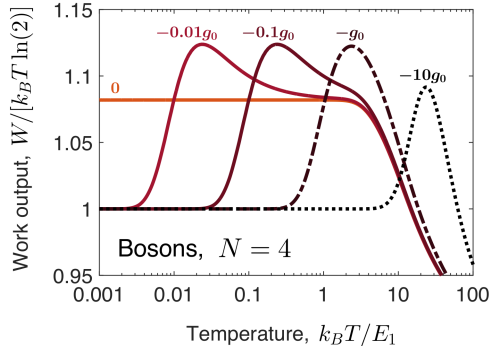


FIG. 4. **Temperature dependence of the work output for  $N = 4$  bosons.** With increasing interaction strength, the peak in the relative work output occurs at a higher temperature, similar to what was shown in Fig. 1(c) for  $N = 3$ .

For classical particles, the optimal work output is given by

$$\begin{aligned}
 W_{\text{tot}} = & -Nk_B T \left[ \left( \frac{\ell^{\text{ins}}}{L} \right)^N \ln \left( \frac{\ell^{\text{ins}}}{L} \right) \right. \\
 & \left. + \left( 1 - \frac{\ell^{\text{ins}}}{L} \right)^N \ln \left( 1 - \frac{\ell^{\text{ins}}}{L} \right) \right] \\
 & - k_B T \sum_{m=1}^{N-1} \binom{N}{m} \left( \frac{\ell^{\text{ins}}}{L} \right)^m \left( 1 - \frac{\ell^{\text{ins}}}{L} \right)^{N-m} \\
 & \times \ln \left[ \frac{\left( \frac{\ell^{\text{ins}}}{L} \right)^m \left( 1 - \frac{\ell^{\text{ins}}}{L} \right)^{N-m}}{\left( \frac{m}{N} \right)^m \left( 1 - \frac{m}{N} \right)^{N-m}} \right]. \quad (12)
 \end{aligned}$$

A numerical scan of different insertion positions shows that an asymmetric insertion point  $\ell^{\text{ins}} \neq L/2$  (as shown by the blue dashed line in Fig. 5) provides the highest work output. In contrast, the symmetric position is optimal for  $N \leq 3$  classical particles. For the non-repulsively interacting bosons

( $g \leq 0$ ) studied here, the symmetric insertion is favorable in the low temperature limit as thoroughly discussed in the main article. On the other hand, for large temperatures the classical result needs to be recovered. This occurs via a pitchfork bifurcation[36] at an intermediate temperature as shown in Fig. 5. For noninteracting Bosons it occurs at  $k_B T_c \approx 50 E_1$  for  $N = 4$ , and at slightly larger values if attractive interactions are included.

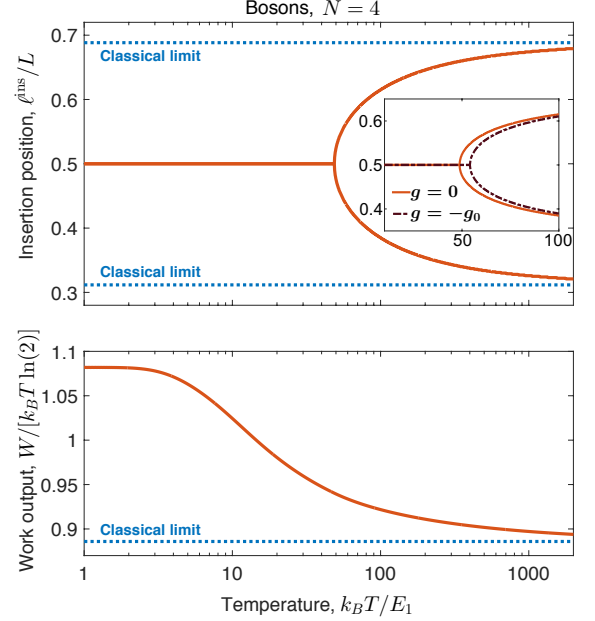


FIG. 5. **Pitchfork bifurcation for the optimal insertion position at a critical temperature for  $N = 4$  bosons.** For large temperatures, the optimal insertion position becomes asymmetric in order to recover the classical result (blue dashed line). The full red line shows the case without interactions  $g = 0$ . The inset in the upper panel shows the corresponding result for  $g = -g_0$  (dark-red lines).